Nuclear magnetic moment of the neutron-rich nucleus ^{21}O

Y. Ishibashi,[1,2,*] A. Gladkov,[1,†] Y. Ichikawa,[1,‡] A. Takamine,[1] H. Nishibata,[1,‡] T. Sato,[1,§] H. Yamazaki,[1] T. Abe,[1] J. M. Daugas,[3,1,∥] T. Egami,[4,1] T. Fujita,[5,1] G. Georgiev,[6,¶] K. Imamura,[7,1] T. Kawaguchi,[4,1] W. Kobayashi,[4,1] Y. Nakamura,[7,1] A. Ozawa,[2] M. Sanjo,[4,1] N. Shimizu,[8,**] D. Tominaga,[4,1] L. C. Tao,[9,1] K. Asahi,[1] and H. Ueno[1]

[1]RIKEN Nishina Center for Accelerator-Based Science, 2-1 Hirosawa, Wako, Saitama 351-0198, Japan
[2]Institute of Physics, University of Tsukuba, 1-1-1 Tennodai, Tsukuba, Ibaraki 305-8571, Japan
[3]CEA, DAM, DIF, F-91297 Arpajon, France
[4]Department of Physics, Hosei University, 2-17-1 Fujimi, Chiyoda-ku, Tokyo 102-8160, Japan
[5]Department of Physics, Osaka University, 1-1 Yamadaoka, Suita, Osaka 656-0871, Japan
[6]CSNSM, CNRS/IN2P3, Université Paris-sud, F-91405 Orsay, France
[7]Department of Physics, Meiji University, 1-1-1 Higashi-Mita, Tama, Kawasaki, Kanagawa, 214-8571, Japan
[8]Center for Nuclear Study, University of Tokyo, Wako Branch at RIKEN, 2-1 Hirosawa, Wako, Saitama 351-0198, Japan
[9]School of Physics, Peking University, Yiheyuan Road Haidian District, Beijing 100871, China

(Received 24 August 2022; accepted 29 November 2022; published 10 February 2023)

The ground-state magnetic dipole moment of the neutron-rich ^{21}O isotope has been measured via β-ray-detected nuclear magnetic resonance (β-NMR) spectroscopy by using a spin-polarized secondary beam of ^{21}O produced from the ^{22}Ne primary beam. From the present measurement, the g factor $|g_{\rm exp}(^{21}{\rm O}_{\rm g.s.})| = 0.6036(14)$ has been determined. Based on the comparison of this value with Schmidt values, we unambiguously confirm the $\nu d_{5/2}$ configuration with spin and parity assignments $I^\pi = 5/2^+$ for the ^{21}O ground state, suggested by previously reported studies. Consequently, the magnetic moment has been determined as $\mu_{\rm exp}(^{21}{\rm O}_{\rm g.s.}) = (-)1.5090(35)\mu_N$. The obtained experimental magnetic moment is in good agreement with the predictions of the shell-model calculations using the USD, YSOX, and SDPF-M interactions as well as random phase approximation (RPA) calculations. This observation indicates that the ^{21}O nucleus in its ground state does not manifest any anomalous structure and is not influenced by the proximity of the drip line.

DOI: 10.1103/PhysRevC.107.024306

I. INTRODUCTION

In the light nuclear region, structural changes have been observed due to the effect of excess neutrons. An interesting phenomenon, the disappearance of conventional magic numbers and the emergence of new magic numbers, such as the neutron numbers $N = 6$, 16, 32, and 34, has been reported [1,2]. Neutron-rich oxygen isotopes are an interesting subject, for which such intriguing properties have been reported. Of particular interest is the anomaly that ^{24}O is a neutron drip line nucleus of the oxygen isotopes. This implies that $N = 16$ is the new magic number [1]. The gap energy spread of $N = 16$ occurs due to the widening energy gap of $1s_{1/2}$ and $0d_{3/2}$ neutron orbits. This double magic property is supported from a recent study on neutron removal reactions of ^{24}O [3]. The even more neutron-rich ^{25}O has also been studied by invariant mass spectroscopy with the two-proton removal reaction of ^{27}Ne [4]. Anomalies in nuclear structure have also been reported for ^{23}O. In a simple shell model, the spin-parity of the ground state of odd-mass neutron-rich oxygen isotopes, including ^{23}O, is $I^\pi = 5/2^+$. Regarding its assignments to ^{23}O, $I^\pi = 5/2^+$ was previously suggested [5], although experiments based on nuclear reactions have concluded that it is $1/2^+$ [6–8]. In addition, consistently with this assignment, spin-parity of $I^\pi = 5/2^+$ for the first excited state measured at $E_{\rm x} = 2.79(13)$ and 2.78(11) MeV has been suggested in studies on both the $2p + 1n$ removal reaction of ^{26}Ne [9] and the $1n$ knockout reaction of ^{24}O [10], respectively. In Ref. [11], excited states were observed at $E_{\rm x} = 4.00(2)$ and 5.30(4) MeV from the ^{22}O(d, p) reaction measurement, with the former characterized as a $d_{3/2}$ single-particle property. To investigate where such structural changes occur in the oxygen isotopes, it is important to investigate the structure of ^{21}O, which is closer to the β-decay stability line than ^{23}O. In contrast to the extensive studies on ^{23}O, however, few attempts have so far been made for ^{21}O. The change in the single-particle energy is indispensable for understanding the

*Present address: Accelerator Engineering Corporation, Konakadai 6-18-1, Inage, Chiba, Chiba 263-0043, Japan.
†Corresponding author: aleksey.gladkov@riken.jp
‡Present address: Department of Physics, Kyushu University, 744 Moto-oka, Nishi, Fukuoka 819-0395, Japan.
§Present address: Institute of Innovative Research, Tokyo Institute of Technology, 2-12-1 Oh-okayama, Meguro, Tokyo 152-8550, Japan.
∥Present address: Université Paris-Saclay, CEA, CNRS, Inserm, SHFJ, BioMaps, 91401 Orsay, France.
¶Present address: IJCLab, CNRS/IN2P3, Université Paris-Saclay, 91405 Orsay, France.
**Present address: Center for Computational Sciences, University of Tsukuba, 1-1-1 Tennodai, Tsukuba, Ibaraki 305-8577, Japan.

structure of neutron-rich nuclei, because it not only affects the position of the neutron drip line, but also changes the nuclear structure, such as the level structure and the configuration mixing of levels. The experimental determination of the spin and parity of the ground state is important to investigate the nuclear structure change, because it is often the starting point of the discussion. From this aspect, theoretical studies on oxygen isotopes include, for example, *ab initio* calculations in recent years (see, for instance, Fig. 3 in Ref. [12] for various *ab initio* results of the ground-state energies).

The structure of ^{21}O has been experimentally investigated through, for instance, the multinucleon transfer reaction [13] and in-beam γ-ray spectroscopy [14], in which $I^{\pi} = 5/2^{+}$ has been tentatively assigned to the ^{21}O ground state. The momentum distribution was measured [6] in the one-neutron removal (knockout) reaction. The same assignment of $I^{\pi} = 5/2^{+}$ as in the previous studies has been claimed. In a more recent study, the $d(^{20}\text{O},^{21}\text{O})p$ reaction as the (d, p) reaction in inverse kinematics was applied for the structure study of ^{21}O [15]. This study also claims the $5/2^{+}$ assignment, because a measured differential cross section to the ^{21}O ground state can be well reproduced with a dominant $l = 2$ component. Recent work has included γ-ray spectroscopic measurements of the low-lying excited state of ^{21}O and the lifetime measurements of the first and second excited states [16]. No particular discrepancies have been reported in comparison with theoretical calculations performed with the assignment of the ground state to $I^{\pi} = 5/2^{+}$. However, according to evaluators [17,18], the $I^{\pi} = 5/2^{+}$ assignment is still treated as a tentative result. In such a situation, it was important to investigate the ^{21}O ground state through a g-factor measurement by β-ray-detected nuclear magnetic resonance (β-NMR) spectroscopy, which is a completely different observable from those obtained in nuclear-reaction-based studies.

In the present work, the magnetic moment μ for the ground states of ^{21}O has been measured. The nuclear moments are sensitive to the internal structure of a nucleus, and they thus provide a means to discover the spin anomalies and nuclear deformations. Therefore, nuclear-moment measurements for neutron-rich oxygen isotopes play an important role in revealing the complete picture of the evolution of their nuclear structure. Prior to the present study, the magnetic dipole moments μ (^{13,15,17,19}O) and electric quadrupole moments Q (^{13,17,19}O) have been reported [19–24].

The present paper is organized as follows: in Sec. II, the experimental methods used in the present work are described. The results of the experimental measurements are presented in Sec. III. In Sec. IV, the comparison of the experimental results with the theoretical predictions and the nuclear structure of the ground state of the ^{21}O are discussed. The paper is summarized in Sec. V.

II. EXPERIMENTAL PROCEDURE

The experimental determination of the ground state magnetic moment consists of three stages: (a) production of a spin-polarized secondary beam of ^{21}O; (b) measurements of the magnitude of the produced polarization in order to ensure the optimal experimental conditions for an efficient β-NMR measurement, and (c) actual measurement of the ^{21}O magnetic moment using the β-NMR method with the implementation of the so-called adiabatic fast passage technique. The details of these procedures are provided in the following subsections.

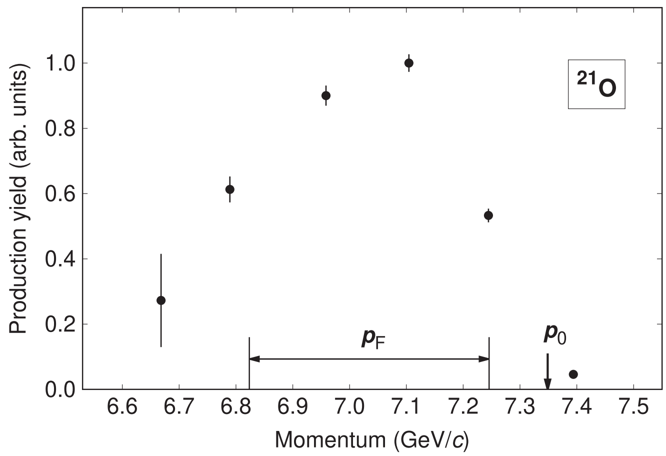

FIG. 1. Momentum distribution of ^{21}O. The momentum window accepted by RIPS for β-NMR measurement is indicated by p_F. p_0 represents the ^{21}O momentum corresponding to the incident beam velocity.

A. Production of spin-polarized ^{21}O beam

The experiment was conducted using the RIKEN projectile fragment separator (RIPS) [25]. The details of the separator layout used to produce the spin-polarized secondary beam can be found in Ref. [26]. A beam of ^{21}O was obtained from the fragmentation of ^{22}Ne projectiles at $E = 70$ MeV/nucleon on a ^{9}Be target of 0.185 g/cm^2 thickness. A well-established method to produce the spin polarization through projectile fragmentation was used [27]. Fragments of ^{21}O emitted at finite angles $\theta_F = (4 \pm 2)^{\circ}$ from the primary beam's direction were accepted by RIPS using a beam swinger installed upstream of the target. In addition, a range of momenta $p_F = p_0 \times (0.96 \pm 0.03)$ was selected by using slits placed at the momentum-dispersive intermediate focal plane. Here, p_0 is the fragment momentum corresponding to the projectile velocity. The measured momentum distribution of ^{21}O is illustrated in Fig. 1.

In the one-neutron pickup reaction in this energy region, it is known from the study of [28] that a large positive nuclear spin polarization is obtained near the peak of the momentum distribution. In addition, for the projectile-fragmentation reaction involving one-neutron pickup, there is an experiment in which ^{34}Al was produced from ^{36}S [29], and a large positive spin-polarization was also obtained near the momentum peak. This phenomenon has been interpreted as the relationship between the momentum-matching condition in the neutron pickup and the corresponding angular momentum left in the fragment. Since the production reaction of ^{21}O in this study is similar to the above-noted ones (in the sense that only single neutron is picked up while the number of protons transferred is even), we selected the region of momenta near the peak, which is indicated in Fig. 1 as p_F.

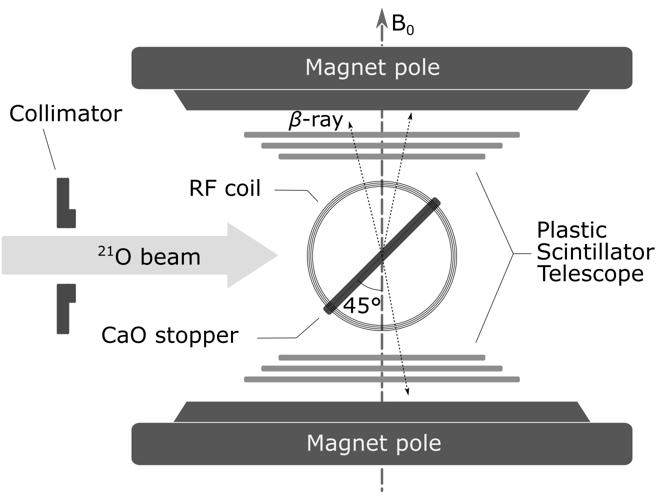

FIG. 2. Schematic view of the β-NMR apparatus. A beam of polarized fragments is introduced as indicated by the arrow. A vertical static magnetic field B_0 is applied with the poles of an iron-core electromagnet. The oscillating magnetic field B_1 is applied perpendicular to B_0 by means of an rf coil in a Helmholtz configuration, which is placed around the stopper crystal. The emitted β rays are detected by the plastic scintillator telescopes located above and below the implantation host.

The isotope-separation was achieved by the combined analyses of the magnetic rigidity and momentum loss in the wedge-shaped degrader [30]. After the separation, the spin-polarized ^{21}O beam was transported to the experimental apparatus described in Fig. 2, which was located at the final focus of the RIPS separator and implanted into a stopper crystal.

B. Spin-polarization measurements

In β-NMR experiments combined with the fragmentation-induced spin polarization, one needs to produce a sufficient size of spin polarization P for ^{21}O to find a resonance; however, upon such a measurement, P can only be known after the resonance is determined. Calculations based on theories at the present stage may not predict with sufficient accuracy the magnitude of polarization, which depends on various factors such as the combination of the projectile and fragment, the projectile energy, the momentum, and the scattering angles of the fragment. For efficient measurements, it is thus necessary to proceed with polarization determination separately, prior to the actual β-NMR spectroscopy. In the present study, we therefore adopted an empirical strategy of performing the polarization (more precisely, $A_\beta P$) measurement based on the adiabatic field rotation (AFR) method [31], where A_β is the asymmetry parameter for the β decay of ^{21}O.

This technique allows us to determine the $A_\beta P$ value [which appears in Eq. (1) below] for the implanted β-radioactive nuclei by adiabatically rotating the strong holding magnetic field provided by permanent Nd magnets by 180° [31], such that the spins of implanted particles "follow" the direction of the external magnetic field, and the sign of polarization is reversed. Thus, the observed change in the β-ray emission asymmetry caused by this spin reversal provides the empirical value for $A_\beta P$. For detailed description of the method and setup arrangement, the reader is referred to [31]. By means of the AFR measurement, the $A_\beta P$ value of ^{21}O was determined as $A_\beta P = 0.90(24)\%$, and the following β-NMR measurements were conducted using the produced spin-polarized ^{21}O beam.

C. Magnetic moment measurements

The magnetic moment of ^{21}O was measured as follows. The spin-polarized ^{21}O nucleus was transported to a β-NMR apparatus located at the final focus of RIPS and implanted into a sintered polycrystalline plate ($28 \times 20 \times 0.5$ mm) of CaO with a cubic crystal structure. The purity of CaO was 99.9%. The spin-lattice relaxation time (T_1) of oxygen in CaO is not known, but the nuclear moments of ^{19}O, whose $T_{1/2} = 27$ s is much longer than the half-life of ^{21}O, have been measured using a CaO crystal [24]. The layout of the β-NMR apparatus is shown in Fig. 2.

A static magnetic field $B_0 = 500.98(16)$ mT was applied to the stopper. This value was obtained by using a weighted average of the magnetic field measured by using an NMR probe several times before and after the measurement. The radio frequency magnetic field B_1 was applied perpendicular to the B_0 by using a coil installed around the CaO stopper crystal.

The β rays emitted from the implanted ^{21}O were detected with plastic scintillator telescopes located above and below the stopper, each consisting of three 1-mm-thick plastic scintillators. The β rays up/down counting ratio R can be written as:

$$R = a\frac{1 + v/c \times A_\beta P}{1 - v/c \times A_\beta P} \simeq a(1 + 2A_\beta P), \qquad (1)$$

where a is a constant representing asymmetries in the counter solid angles ($\Omega_\beta \approx 4\pi \times 0.26$ sr each) and efficiencies, and v/c is the velocity of the β particle relative to the speed of light. Taking into account the energy of the β rays emitted from ^{21}O (i.e., average energy of β rays is 5173 keV [18]), the ratio R in Eq. (1) is well approximated by setting $v/c \approx 1$. The adiabatic fast passage (AFP) technique [32] was implemented in order to realize the reversal of the spin polarization. By taking a double ratio $R/R_{\rm off}$, where $R_{\rm off}$ is the value for R measured without an oscillating magnetic field B_1, the resonance frequency is derived from the position of a peak in the obtained spectrum.

The beam was pulsed with beam-on and beam-off periods of 2 and 8s [$T_{1/2}(^{21}{\rm O}_{\rm g.s.}) = 3.4$ s], respectively. This sequence timing was chosen based on the results of the systematic AFR measurements. In the beam-off period after the beam implantation, the B_1 field was applied for the first 10 ms. Then, the β rays were counted for 8 s, and in the last 10 ms of the beam-off period the B_1 field was applied again to reverse the initial spin direction in order to reduce the effect of the reversed polarization on the subsequent cycles. This measurement procedure was repeated for a particular set of frequencies and concluded with a cycle without the application of the B_1 field, which serves as a baseline in the

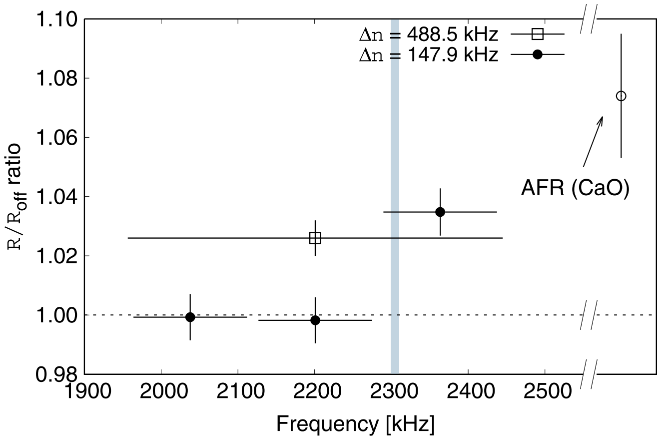

FIG. 3. Wide search β-NMR spectrum. The two separate runs with a single scan frequency sweep of $\Delta\nu = 488.5$ kHz (open square) and $\Delta\nu = 147.9$ kHz (solid circles) are shown. For the definition of $R/R_{\rm off}$ ratio, refer to the text. The result of the AFR measurement is shown by an open circle as a deviation of a fourfold ratio [31] from unity.

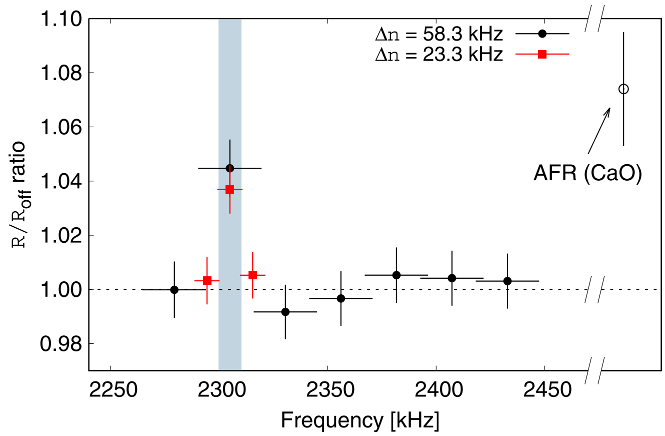

FIG. 4. β-NMR spectrum for ^{21}O in CaO stopper crystal, obtained with finer frequency segmentation. The panel includes the results obtained in two separate runs with a single sweep width of $\Delta\nu = 58.3$ kHz (black circles) and $\Delta\nu = 23.3$ kHz (red squares), where the horizontal bars represent the width of each frequency's sweep. The shaded area shows the assignment of the uncertainty of the deduced Larmor frequency. The result of the AFR measurement is indicated by an open circle.

β-NMR spectrum. The entire sequence was repeated until sufficient statistics were accumulated.

III. RESULTS

The measurement of the g factor for ^{21}O was performed in stages. First, a single wide frequency window scan of $\Delta\nu = 488.5$ kHz was conducted to confirm the presence of the resonance within the selected region and to ensure that the magnitude of the spin polarization was sufficient for the actual g-factor measurement. Here, the frequencies ranging from 1956 to 2445 kHz were scanned, which corresponded to $g = 0.5125$–0.6405. Since the resonance shows up as the change in the β-ray R ratio, the deviation of the double ratio $R/R_{\rm off}$ for this scan from the unity indicates the occurrence of the spin alteration by AFP-NMR, where $R_{\rm off}$ is the R ratio obtained without the B_1 field. This result is also assured by the fact that the obtained $R/R_{\rm off}$ is in agreement with that obtained by the AFR within the error bars. The obtained $R/R_{\rm off}$ value is shown by the open square in Fig. 3, together with the $R/R_{\rm off}$ converted from the $A_\beta P$ value measured by the AFR method. Once the NMR effect was observed, resonance scans with progressively narrower frequency windows $\Delta\nu = 147.9$ and 58.3 kHz were conducted in order to define more precisely the location of the resonance. The obtained β-NMR spectra are shown by solid circles in Figs. 3 and 4, respectively.

We found that only the intervals which included a common value $\nu \approx 2305$ kHz exhibited the NMR effect. Comparing the $A_\beta P$ values obtained by AFR and AFP-NMR, they agree in both Figs. 3 and 4 within the 1.7σ and 1.6σ error bounds, respectively, although the AFR values are slightly larger. Then, a precision frequency scan of $\Delta\nu = 23.3$kHz was performed. The result of this measurement is represented by red squares in Fig. 4. Since there are only three data points, further analysis, such as least-χ^2 fitting, was not performed, and $\nu_{\rm L} = 2304.9 \pm 5.3$ kHz, which simply corresponds to a center frequency and full width of the scanned frequency region for the data points exhibiting resonance, was determined as the experimental resonance frequency (i.e., Larmor frequency). From the obtained $\nu_{\rm L}$, the ground state g factor of ^{21}O was determined as $|g_{\rm exp}(^{21}{\rm O}_{\rm g.s.})| = 0.6036(14)$.

IV. DISCUSSION

Because ^{21}O has a $Z = 8$ proton closed shell, its ground-state spin-parity I^π is dominantly formed by the five neutrons in the *sd* orbits. In a simple shell model, the ground state of ^{21}O is represented by the configuration with one unpaired neutron in the $d_{5/2}$ orbit, i.e., $|[(\nu sd)^4]^{0^+}(\nu d_{5/2})\rangle^{I^\pi=5/2^+}$ (where the main components of $[(\nu sd)^4]^{0^+}$ will be $[(\nu d_{5/2})^4]^{0^+}$, $[(\nu d_{5/2})^2(\nu s_{1/2})^2]^{0^+}$, or the admixture thereof). In this configuration, the ground-state spin-parity becomes $I^\pi = 5/2^+$, similar to the odd-mass neutron-rich oxygen isotopes ^{17}O and ^{19}O, which also have one unpaired neutron in the $d_{5/2}$ orbit.

The neighboring nuclei of ^{21}O with even-Z number nearest to $Z = 8$ and the same neutron number $N = 13$ are ^{23}Ne and ^{19}C, whose spin-parities are also formed by the five neutrons in the *sd* orbits. Interestingly, however, their spin-parities are different from each other: $I^\pi(^{23}{\rm Ne}_{\rm g.s.}) = 5/2^+ (Z = 10)$ and $I^\pi(^{19}{\rm C}_{\rm g.s.}) = 1/2^+ (Z = 6)$ [33]. Provided the neutron configuration of ^{21}O is approximately the same as ^{23}Ne, which is natural in a simple shell model, $I^\pi = 5/2^+$ is suggested for the ^{21}O ground state. However, if ^{21}O neutrons are in the same situation as in the case of ^{19}C, the $I^\pi = 1/2^+$ assignment is also possible.

Here, we consider two possible configurations in which an unpaired $d_{5/2}$ or $s_{1/2}$ neutron carries the nuclear spin-parity $I^\pi = 5/2^+$ or $1/2^+$, respectively. Then, the g factors corresponding to the possible two configurations $|[(\nu sd)^4]^{0^+}(\nu d_{5/2})\rangle^{I^\pi=5/2^+}$ and $|[(\nu sd)^4]^{0^+}(\nu s_{1/2})\rangle^{I^\pi=1/2^+}$, calculated with the bare g factors are provided as $g_{\rm Schmidt}(\nu d_{5/2}) = -0.765$ and $g_{\rm Schmidt}(\nu s_{1/2}) = -3.826$,

TABLE I. Comparison of experimental magnetic moments $\mu_{\mathrm{exp}}(^{21}\mathrm{O})$ obtained for the ^{21}O ground state in the present study with shell-model (USD, YSOX, and SDPF-M) and RPA (D1S and D1M) predictions. The $\mu_{\mathrm{exp}}(^{21}\mathrm{O})$ was calculated from the determined $|g_{\mathrm{exp}}(^{21}\mathrm{O})|$ factor and the assigned $I^{\pi} = 5/2^{+}$. The Schmidt moment (μ_{Schmidt}) for a $d_{5/2}$ neutron is also illustrated.

	μ moment (μ_N)
$\mu_{\mathrm{exp}}(^{21}\mathrm{O})$	(−)1.5090(35)
μ_{Schmidt}	−1.913
USD	−1.44
YSOX	−1.402
SDPF-M	−1.476
RPA(D1S)	−1.667
RPA(D1M)	−1.487

respectively. Although a sign was not assigned to the experimental g factors determined in the present study, i.e., $|g_{\mathrm{exp}}(^{21}\mathrm{O}_{\mathrm{g.s.}})| = 0.6036(14)$, we can assign $I^{\pi} = 5/2^{+}$ to the ^{21}O ground state even if it is only from the comparison of the absolute value to the above-noted Schmidt values, due to the large difference in $g_{\mathrm{Schmidt}}(\nu d_{5/2})$ and $g_{\mathrm{Schmidt}}(\nu s_{1/2})$.

It is also interesting to compare the $|g_{\mathrm{exp}}(^{21}\mathrm{O}_{\mathrm{g.s.}})|$ value with the g factors of the neighboring nuclei, ^{17}O and ^{19}O, whose ground state I^{π} are known to be $5/2^{+}$. The experimental g factors for $|g_{\mathrm{exp}}(^{17}\mathrm{O}_{\mathrm{g.s.}})| = |-0.75752(4)|$ [22] and $|g_{\mathrm{exp}}(^{19}\mathrm{O}_{\mathrm{g.s.}})| = 0.61278(3)$ [24] are close to the present $|g_{\mathrm{exp}}(^{21}\mathrm{O}_{\mathrm{g.s.}})|$ value in comparison to their absolute values. This suggests the assignment of $I^{\pi}(^{21}\mathrm{O}_{\mathrm{g.s}}) = 5/2^{+}$. Thus, the ground-state nuclear magnetic moment of ^{21}O can be determined as $\mu_{\mathrm{exp}}(^{21}\mathrm{O}_{\mathrm{g.s.}}) = (-)1.5090(35)\mu_N$ [hereafter $\mu_{\mathrm{exp}}(^{21}\mathrm{O}_{\mathrm{g.s.}})$ will be assigned a negative sign from the above $I^{\pi} = 5/2^{+}$ assignment in the comparison with theoretical values].

The admixture of proton-excited configurations in ^{21}O is suppressed due to the *LS*-closed ^{16}O core. Thus, the effect of configuration mixing is approximately caused only by the neutron's side. In this situation, the wave function of $^{21}\mathrm{O}_{\mathrm{g.s.}}$ can be approximately written in the seniority scheme as follows:

$$\begin{aligned}\psi\left(^{21}\mathrm{O}_{\mathrm{g.s}}\right) &= c_0|[(\nu sd)^4]^{0^+}(\nu d_{5/2})\rangle^{I^{\pi}=5/2^+} \\ &\quad + c_1|[(\nu sd)^2]^{0^+}[(\nu d_{5/2})(\nu d_{3/2})]^{J^+}(\nu d_{5/2})\rangle^{I^{\pi}=5/2^+} \\ &\quad + \cdots \\ &\qquad \left(c_0{}^2 + c_1{}^2 + \cdots = 1\right), \end{aligned} \tag{2}$$

where the c_0 term corresponds to the seniority 1, the c_1 term to the seniority 3 [consisting of the seniority 2, $[(\nu d_{5/2})(\nu d_{3/2})]^{J^+}$, and the seniority 1, $(\nu d_{5/2})$], and so on. Note that J can take any values possible for the intermediate states. To discuss the ground-state configuration of ^{21}O, based on Eq. (2), the $\mu_{\mathrm{exp}}(^{21}\mathrm{O}_{\mathrm{g.s.}})$ value was compared with the results of the shell-model calculation with the USD interaction [34] conducted utilizing the KSHELL code [35], as provided in Table I. The calculated μ value was $\mu_{\mathrm{USD}} = -1.44\mu_N$, where we adopted the effects of the meson exchange currents and effective g factors of [36]. The difference from the experimental value was only $\delta\mu \simeq 0.07\mu_N$, suggesting that ^{21}O is well described as a "normal" nucleus. The amplitude of each configuration in Eq. (2) was calculated to be $|c_0|^2 \simeq 90\%$, and $|c_1|^2 \simeq 1.6\%$. The dominant c_0 component gives a single-particle μ moment of $\nu d_{5/2}$, but the c_1 term with $J^{+} = 1^{+}$ causes quenching of the effect of off-diagonal $M1$ matrix elements with the c_0 term [37]. The observed $\delta\mu \simeq 0.4$ is mainly explained by such effects. We note that calculations with the USDA and USDB interactions [38] were also conducted in addition to USD, where the maximum difference among them was only $\delta\mu \leqslant 0.05\mu_N$.

This observation is supported also by the shell-model calculations in model spaces larger than the *sd* shell. Here, we performed the calculations in the *psd* and *sdpf* model spaces with the YSOX [39] and the SDPF-M [40] interactions, respectively. As shown in Table I, the μ moments calculated in the *psd* and *sdpf* shells are similar to those in the *sd* shell with the USD interactions. Note that the free nucleon g factors were adopted in the calculations. The results with the YSOX interaction provide that the percentage of the excitations from the p to the *sd* shell is approximately 16.8%. With the SDPF-M interaction, the percentage of the excitations from the *sd* to the *pf* shell is evaluated as approximately 0.5%. From these results in the *psd* and *sdpf* shells, the shell-model description in the *sd* shell is sufficient to explain the $\mu_{\mathrm{exp}}(^{21}\mathrm{O}_{\mathrm{g.s.}})$ moment, suggesting the ground state of ^{21}O is "normal" from a single-particle point of view.

Besides the discussion above, a nuclear-structure study of the ^{21}O ground state based on the random phase approximation (RPA) has been reported also [41], where the polarization effect of the doubly-magic core in odd-even nuclei was described using a single-particle basis generated by Hartree-Fock calculations. The $\mu_{\mathrm{exp}}(^{21}\mathrm{O}_{\mathrm{g.s.}})$ is in good agreement with the predicted ones, $\mu_{\mathrm{RPA(D1S)}} = -1.667\mu_N$ and $\mu_{\mathrm{RPA(D1M)}} = -1.487\mu_N$, calculated using two different parametrizations of the finite-range density-dependent Gogny interactions based on the traditional D1S force [42] and the recently proposed D1M one [43], respectively, taking ^{22}O as a core coupled with a $\nu d_{5/2}$ hole. When comparing the two calculations, the reduction in μ from the $\nu d_{5/2}$ single-particle moment will be insufficient for $\mu_{\mathrm{RPA(D1S)}}$.

V. SUMMARY

In the present study, the magnetic moment of the ground state of ^{21}O was measured by using the β-NMR method with a spin-polarized radioactive isotope beam. In the experiment, the production of the spin polarized ^{21}O beam was confirmed using the adiabatic-field-rotation method and β-NMR spectroscopy was conducted. As a result of the measurement, the experimental g factor for the ^{21}O ground state has been determined as $|g_{\mathrm{exp}}(^{21}\mathrm{O}_{\mathrm{g.s.}})| = 0.6036(14)$. Based on the comparison of the thus determined g factor with the single-particle g factors of the neutrons in the $d_{5/2}$ and $s_{1/2}$ orbits, we firmly confirmed the previously suggested assignment [17] of $I^{\pi} = 5/2^{+}$ to the ^{21}O ground state. Owing to the definite assignment of $I^{\pi}(^{21}\mathrm{O}_{\mathrm{g.s.}})$, we determined its magnetic moment as $\mu_{\mathrm{exp}}(^{21}\mathrm{O}_{\mathrm{g.s.}}) = (-)1.5090(35)\mu_N$. In the comparison of the experimental μ moment with shell-model calculations as well as with the RPA calculations, a good agreement is found.

From this observation, we concluded that the ^{21}O nucleus does not manifest any anomalous structure in the ground state and is not influenced by the proximity of the drip line.

ACKNOWLEDGMENTS

The authors would like to thank the staff of the RIKEN Ring Cyclotron for their support during the experiment. The author Y.I. is grateful for support from the Junior Research Associate Program in RIKEN. This experiment was conducted at the RI Beam Factory operated by RIKEN Nishina Center for Accelerators-based Science and CNS, University of Tokyo, under Experimental Program ML1602-RRC43. This project was supported by JSPS and CNRS under the Japan-France Research Cooperative Program, and by MEXT/JSPS KAKENHI Grants No. 18H03692 and No. 18H05462.

[1] A. Ozawa, T. Kobayashi, T. Suzuki, K. Yoshida, and I. Tanihata, Phys. Rev. Lett. **84**, 5493 (2000).

[2] D. Steppenbeck, S. Takeuchi, N. Aoi, P. Doornenbal, M. Matsushita, H. Wang, H. Baba, N. Fukuda, S. Go, M. Honma, J. Lee, K. Matsui, S. Michimasa, T. Motobayashi, D. Nishimura, T. Otsuka, H. Sakurai, Y. Shiga, P. A. Söderström, T. Sumikama *et al.*, Nature (London) **502**, 207 (2013).

[3] D. A. Divaratne, C. R. Brune, H. N. Attanayake, T. Baumann, D. Bazin, A. Gade, S. M. Grimes, P. M. King, M. Thoennessen, and J. A. Tostevin, Phys. Rev. C **98**, 024306 (2018).

[4] C. Sword, J. Brett, T. Baumann, B. A. Brown, N. Frank, J. Herman, M. D. Jones, H. Karrick, A. N. Kuchera, M. Thoennessen, J. A. Tostevin, M. Tuttle-Timm, and P. A. DeYoung, Phys. Rev. C **100**, 034323 (2019).

[5] R. Kanungo, M. Chiba, N. Iwasa, S. Nishimura, A. Ozawa, C. Samanta, T. Suda, T. Suzuki, T. Yamaguchi, T. Zheng, and I. Tanihata, Phys. Rev. Lett. **88**, 142502 (2002).

[6] E. Sauvan, F. Carstoiu, N. A. Orr, J. S. Winfield, M. Freer, J. C. Angélique, W. N. Catford, N. M. Clarke, M. MacCormick, N. Curtis, S. Grévy, C. LeBrun, M. Lewitowicz, E. Liégard, F. M. Marqués, P. Roussel-Chomaz, M.-G. Saint Laurent, and M. Shawcross, Phys. Rev. C **69**, 044603 (2004).

[7] D. Cortina-Gil, J. Fernandez-Vazquez, T. Aumann, T. Baumann, J. Benlliure, M. J. G. Borge, L. V. Chulkov, U. Datta Pramanik, C. Frossén, L. M. Fraile, H. Geissel, J. Gerl, F. Hammache, K. Itahashi, R. Janik, B. Jonson, S. Mandal, K. Markenroth, M. Meister, M. Mocko *et al.*, Phys. Rev. Lett. **93**, 062501 (2004).

[8] C. Nociforo, K. L. Jones, L. H. Khiem, P. Adrich, T. Aumann, B. V. Carlson, D. Cortina-Gil, U. D. Pramanik, T. W. Elze, H. Emling, H. Geissel, M. Hellström, J. V. Kratz, R. Kulessa, T. Lange, Y. Leifels, H. Lenske, E. Lubkiewicz, G. Münzenberg, R. Palit *et al.*, Phys. Lett. B **605**, 79 (2005).

[9] A. Schiller, N. Frank, T. Baumann, D. Bazin, B. A. Brown, J. Brown, P. A. DeYoung, J. E. Finck, A. Gade, J. Hinnefeld, R. Howes, J.-L. Lecouey, B. Luther, W. A. Peters, H. Scheit, M. Thoennessen, and J. A. Tostevin, Phys. Rev. Lett. **99**, 112501 (2007).

[10] K. Tshoo, Y. Satou, C. A. Bertulani, H. Bhang, S. Choi, T. Nakamura, Y. Kondo, S. Deguchi, Y. Kawada, Y. Nakayama, K. N. Tanaka, N. Tanaka, Y. Togano, N. Kobayashi, N. Aoi, M. Ishihara, T. Motobayashi, H. Otsu, H. Sakurai, S. Takeuchi *et al.*, J. Phys. G: Nucl. Part. Phys. **47**, 055113 (2020).

[11] Z. Elekes, Z. Dombradi, N. Aoi, S. Bishop, Z. Fulop, J. Gibelin, T. Gomi, Y. Hashimoto, N. Imai, N. Iwasa, H. Iwasaki, G. Kalinka, Y. Kondo, A. A. Korsheninnikov, K. Kurita, M. Kurokawa, N. Matsui, T. Motobayashi, T. Nakamura, T. Nakao *et al.*, Phys. Rev. Lett. **98**, 102502 (2007).

[12] K. Hebeler, J. D. Holt, J. Menéndez, and A. Schwenk, Annu. Rev. Nucl. Part. Sci. **65**, 457 (2015).

[13] W. N. Catford, L. K. Fifield, N. A. Orr, and C. L. Woods, Nucl. Phys. A **503**, 263 (1989).

[14] M. Stanoiu, F. Azaiez, Z. Dombrádi, O. Sorlin, B. A. Brown, M. Belleguic, D. Sohler, M. G. Saint Laurent, M. J. Lopez-Jimenez, Y. E. Penionzhkevich, G. Sletten, N. L. Achouri, J. C. Angélique, F. Becker, C. Borcea, C. Bourgeois, A. Bracco, J. M. Daugas, Z. Dlouhý, C. Donzaud *et al.*, Phys. Rev. C **69**, 034312 (2004).

[15] B. Fernández-Domínguez, J. S. Thomas, W. N. Catford, F. Delaunay, S. M. Brown, N. A. Orr, M. Rejmund, M. Labiche, M. Chartier, N. L. Achouri, H. A. Falou, N. I. Ashwood, D. Beaumel, Y. Blumenfeld, B. A. Brown, R. Chapman, N. Curtis, C. Force, G. de France, S. Franchoo *et al.*, Phys. Rev. C **84**, 011301(R) (2011).

[16] S. Heil, M. Petri, K. Vobig, D. Bazin, J. Belarge, P. Bender, B. A. Brown, R. Elder, B. Elman, A. Gade, T. Haylett, J. D. Holt, T. Hüther, A. Hufnagel, H. Iwasaki, N. Kobayashi, C. Loelius, B. Longfellow, E. Lunderberg, M. Mathy *et al.*, Phys. Lett. B **809**, 135678 (2020).

[17] Evaluated Nuclear Structure Data File Search and Retrieval (ENSDF), http://www.nndc.bnl.gov/ensdf/.

[18] R. B. Firestone, Nucl. Data Sheets **127**, 1 (2015).

[19] K. Matsuta, T. Minamisono, M. Tanigaki, M. Fukuda, Y. Nojiri, M. Mihara, T. Onishi, T. Yamaguchi, A. Harada, M. Sasaki, T. Miyake, K. Minamisono, T. Fukao, K. Sato, Y. Matsumoto, T. Ohtsubo, S. Fukuda, S. Momota, K. Yoshida, A. Ozawa *et al.*, Hyperfine Interact. **97-98**, 519 (1996).

[20] K. Matsuta, K. Sato, M. Fukuda, M. Mihara, T. Yamaguchi, M. Sasaki, T. Miyake, K. Minamisono, T. Minamisono, M. Tanigaki, T. Ohtsubo, T. Onoshi, Y. Nojiri, S. Momota, S. Fukuda, K. Yoshida, A. Ozawa, T. Kobayashi, I. Tanihata, J. R. Alonso *et al.*, Phys. Lett. B **459**, 81 (1999).

[21] M. Tanigaki, M. Matsui, M. Mihara, M. Mori, M. Tanaka, T. Yanagisawa, T. Ohtsubo, T. Izumikawa, A. Kitagawa, M. Fukuda, K. Matsuta, Y. Nojiri, and T. Minamisono, Hyperfine Interact. **78**, 105 (1993).

[22] F. Alder and F. C. Yu, Phys. Rev. **81**, 1067 (1951).

[23] H. F. Schaefer, R. A. Klemm, and F. E. Harris, Phys. Rev. **181**, 137 (1969).

[24] T. Minamisono, Y. Nojiri, K. Matsuta, M. Fukuda, K. Sato, M. Tanigaki, A. Morishita, T. Miyake, Y. Matsumoto, T. Onishi, K. Ishiga, F. Ohsumi, H. Kitagawa, and H. Sagawa, Phys. Lett. B **457**, 9 (1999).

[25] T. Kubo, M. Ishihara, N. Inabe, H. Kumagai, I. Tanihata, K. Yoshida, T. Nakamura, H. Okuno, S. Shimoura, and K. Asahi, Nucl. Instrum. Methods Phys. Res., Sect. B **70**, 309 (1992).

[26] H. Ueno, K. Asahi, H. Izumi, K. Nagata, H. Ogawa, A. Yoshimi, H. Sato, M. Adachi, Y. Hori, K. Mochinaga, H. Okuno, N. Aoi,

M. Ishihara, A. Yoshida, G. Liu, T. Kubo, N. Fukunishi, T. Shimoda, H. Miyatake, M. Sasaki *et al.*, Phys. Rev. C **53**, 2142 (1996).

[27] K. Asahi, M. Ishihara, N. Inabe, T. Ichihara, T. Kubo, M. Adachi, H. Takanashi, M. Kouguchi, M. Fukuda, D. Mikolas, D. Morrissey, D. Beaumel, T. Shimoda, H. Miyatake, and N. Takahashi, Phys. Lett. B **251**, 488 (1990).

[28] D. E. Groh, P. F. Mantica, A. E. Stuchbery, A. Stolz, T. J. Mertzimekis, W. F. Rogers, A. D. Davies, S. N. Liddick, and B. E. Tomlin, Phys. Rev. Lett. **90**, 202502 (2003).

[29] K. Turzo, P. Himpe, D. L. Balabanski, G. Belier, D. Borremans, J. M. Daugas, G. Georgiev, F. de Oliveira Santos, S. Mallion, I. Matea, G. Neyens, Y. E. Penionzhkevich, C. Stodel, N. Vermeulen, and D. Yordanov, Phys. Rev. C **73**, 044313 (2006).

[30] T. Minamisono, Hyperfine Interact. **35**, 979 (1987).

[31] Y. Ishibashi, N. Yoshida, H. Ueno, A. Yoshimi, Y. Ichikawa, Y. Abe, K. Asahi, M. Chikamori, T. Fujita, T. Furukawa, E. Hikota, D. Nagae, Y. Ohtomo, Y. Saito, H. Shirai, T. Suzuki, X. Yang, and N. Sakamoto, Nucl. Instrum. Methods Phys. Res., Sect. B **317**, 714 (2013).

[32] A. Abragam, *The Principles of Nuclear Magnetism* (Oxford University Press, Oxford, 1961).

[33] T. Nakamura, N. Fukuda, T. Kobayashi, N. Aoi, H. Iwasaki, T. Kubo, A. Mengoni, M. Notani, H. Otsu, H. Sakurai, S. Shimoura, T. Teranishi, Y. X. Watanabe, K. Yoneda, and M. Ishihara, Phys. Rev. Lett. **83**, 1112 (1999).

[34] B. H. Wildenthal, Prog. Part. Nucl. Phys. **11**, 5 (1984).

[35] N. Shimizu, T. Mizusaki, T. Utsuno, and Y. Tsunoda, Comput. Phys. Commun. **244**, 372 (2019).

[36] B. A. Brown and B. H. Wildenthal, Nucl. Phys. A **474**, 290 (1987).

[37] H. Noya, A. Arima, and H. Horie, Prog. Theor. Phys. Suppl. **8**, 33 (1958).

[38] B. A. Brown and W. A. Richter, Phys. Rev. C **74**, 034315 (2006).

[39] C. Yuan, T. Suzuki, T. Otsuka, F. Xu, and N. Tsunoda, Phys. Rev. C **85**, 064324 (2012).

[40] Y. Utsuno, T. Otsuka, T. Mizusaki, and M. Honma, Phys. Rev. C **60**, 054315 (1999).

[41] G. Co', V. De Donno, M. Anguiano, R. N. Bernard, and A. M. Lallena, Phys. Rev. C **92**, 024314 (2015).

[42] J. F. Berger, M. Girod, and D. Gogny, Comput. Phys. Commun. **63**, 365 (1991).

[43] S. Goriely, S. Hilaire, M. Girod, and S. Péru, Phys. Rev. Lett. **102**, 242501 (2009).